Scientific Visualization, 2023, volume 15, number 4, pages 124 - 139, DOI: 10.26583/sv.15.4.10

Estimation of Sheet Deformation of Aluminium Blank using Non-Contact Methods on the Example of Erichsen Cupping Test

M.A. Petrov[1,A], D.A. Romashov[2,A], V.V. Isakov[3,B]

[A] FSAEI HE «Moscow Polytechnic University»
[B] Central Institute of Aviation Motors

[1] ORCID: 0000-0002-2324-5057, petrovma_mospolytech@mail.ru
[2] ORCID: 0009-0006-3210-464X, dimaromashov393@gmail.com
[3] ORCID: 0009-0001-4955-4835, vvisakov@ciam.ru

Abstract

In the present study, non-contact techniques for estimating the deformation of a sheet specimen of aluminium alloy AA5051 (AMg2) subjected to Erichsen cupping test are considered. It is shown that it is possible to get reliable information by numerical simulation, however, for the case when the coefficients of the yield and fracture equations of the material are well-known and validated. This requires the application of confirmatory techniques based on the results of real experiments, for example, through optical 3D-scanning. The realization of the techniques requires preparing the blank prior the experimental stage. The combined technique of speckle interferometry and digital image correlation allows estimating deformations on the outer linear surfaces, but does not indicate deformations of products with curved surfaces and inside the specimen, which requires performing an additional numerical simulation.

Keywords: AA5051, sheet forming, AI, FEM, DIC, QForm, 3D-scanning.

1. Introduction

The following methods of estimating the true or logarithmic deformation during sheet metal drawing are used in the practice of material forming: by means of moiré strips, deformed grids and strain gauges, polarization-optical and by means of hardness measurements. These methods are divided into two large groups: contact methods, i.e. methods in which the strain is calculated either by measuring the displacement of a point with measuring tools or requiring special sensors (e.g. strain gauges), and non-contact methods, i.e. methods in which the strain is calculated on the basis of the obtained optical information.

Measuring the deformation during a sheet metal forming process, such as drawing, at each point of the material being deformed is a complex task. The metal sheet undergoes not only deformation in the sheet plane, but also in thickness, as a result of thinning and thickening. Figure 1 shows commercially produced sheet metal representative parts.

With the development of computer methods for simulation of sheet metal forming processes, it has become much easier to evaluate their deformation. The use of computer programs instead of theoretical calculations is due to the variety of combined problems, each of which requires a large set of theoretical formulas. Programs based on the finite element method (FEM) are devoid of this and solve the problem on the basis of data on, for example, displacements and velocities at the nodal points of the finite element mesh, which is used to discretize the object under study. On the basis of the obtained results the design of the tool forming surface is taken place, which today can be performed both by traditional approaches and by solving the optimization problem of the non-forming surfaces, for example, by topological optimization algorithms, which help to reduce the tool mass saving their rigidity [4-8].

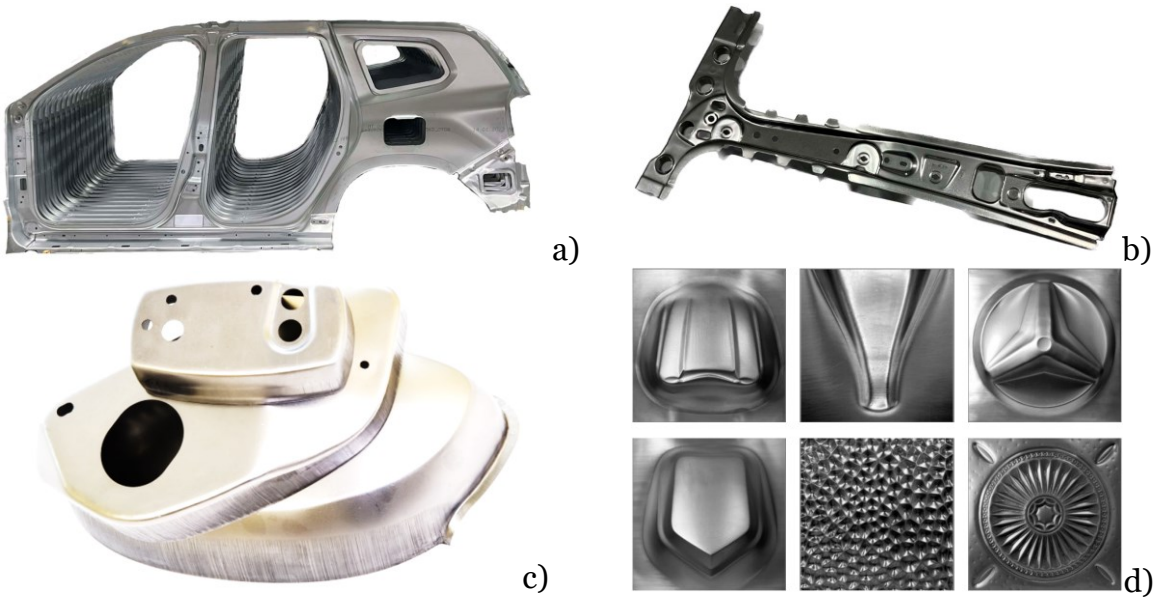

Fig. 1. Examples of the metallic sheet parts: vehicle body side part (a) and B-pillar (b) [1], housing part (c) [2] and special application parts (d) [3]

There is a sufficiently great number of Russian and foreign works, in which the deformation of materials is assessed in a non-contact manner, during mechanical tests, with further plotting flow curves, forming limit diagrams, etc. Many works contain the research on the application of non-contact strain assessment systems: to collect data on material behavior for subsequent accurate computer simulation of sheet material fracture under different loading conditions (uniaxial tension, bulging test according to standard ISO 16808:2022) [9]; for capturing strains of sandwich structure based on steel sheet and glass fiber [10]; to measure the strain of carbon fiber-reinforced plastic specimens according to GOST R 56799–2015 [11]; to clarify the macroscopic localization of non-uniform plastic flow as a result of the Portevin-Le Chatelier effect of aluminum specimens at different stress-strain states (SSS) [12, 13]; to obtain information on the ultimate forming curve by the Marcignac method, according to the standard ISO ISO-12004-2-2021 [14]; for determining critical strain values in uniaxial tension of steel specimens with stress concentrators [15], for determining the strain field when testing composite materials based on glass-textolite and carbon fiber-reinforced plastic under uniaxial tensile pattern [16]. Based on non-contact algorithms of strain estimation, a system can be developed to determine the micro- and macro-architectonics of the surface based on captures of the surface of a welded stainless steel specimen subjected to fatigue testing [17]. The use of non-contact systems hides a number of peculiarities, for example, when the part's geometry is complex and the material is heterogeneous, the material is a sandwich-like structure, i.e. a combination of metal sheet and polymer adhesive bonding, e.g. motor fan housing [18]. When deforming such a material, measurement error may occur due to inhomogeneity of temperature distribution along the material thickness due to different thermophysical values of material properties, and the ultimate deformation of layers and their subsequent delamination may remain undetected.

2. Theoretical formulation of deformation term

Logarithmic strain refers to the natural logarithm of the ratio of the final size to the initial size, Eq. (1), and, according to the law of equality of the volume of the body before and after deformation, the sum of strains along three directions is equal to zero, the Eq. (2) [19]. Thus, if we know the value of deformation in one of the three directions, then the value of deformations in the second and third directions can be determined by theoretical dependence, for example, by the Eq. (3), for the case of axisymmetric cup drawing.

$$\varepsilon = \ln\left(\frac{\dim}{\dim_o}\right), \tag{1}$$

$$\sigma_\rho + \sigma_\theta + \sigma_z = 0, \tag{2}$$

$$\left.\begin{aligned}&\sigma_\rho + \sigma_\theta + \sigma_z = 0\\ &\frac{\sigma_\rho}{\sigma_\theta} = \frac{\varepsilon_\rho - \varepsilon_z}{\varepsilon_\theta - \varepsilon_z}\end{aligned}\right\} \Rightarrow \frac{\sigma_\rho}{\sigma_\theta} =$$

$$= -\frac{\varepsilon_\theta + 2\varepsilon_z}{\varepsilon_\theta - \varepsilon_z} = \left(\ \right] \ \frac{\sigma_\rho}{\sigma_\theta} = a\right) \Rightarrow \tag{3}$$

$$\Rightarrow \varepsilon_z = -\frac{1+a}{2-a}\varepsilon_\theta,$$

where dim_o and dim – initial and end dimensions of the investigated object; $\sigma_\rho, \sigma_\theta, \sigma_z$ – radial stress, circumferential stress and longitudinal stress, respectively; $\varepsilon_\rho, \varepsilon_\theta, \varepsilon_z$ – radial strain, circumferential strain and longitudinal strain, respectively.

3. Applicability of artificial intelligence in technological process design

Given the current global trends in mechanical testing and measurement techniques, more and more research activities is being done on non-contact methods of strain assessment with the incorporation of artificial intelligence algorithms. There are several levels: neural networks (NN), deep learning (DL), machine learning (ML) and artificial intelligence (AI), in the narrow and broad sense. According to the modern terminology, each level includes the previous one, with the highest level being artificial intelligence and the lowest or basic level being neural networks [20]**Ошибка! Источник ссылки не найден.**. At the DL stage, the machine is trained by searching for the best algorithm, without human assistance. At the ML stage, the machine actively uses all kinds of existing databases (DB), and at the AI stage, the solution is created completely without human participation, by the machine itself.

It is quite possible to assume that the application of AI in process design is possible and expected, as a lot of practical experience has been accumulated and can be used in ML, algorithms of NN have been developed, including convolutional NN, deep trust NN, generative adversarial NN, recurrent NN, Boltzmann machine or stochastic recurrent NN and others.

The algorithm of AI block implementation may look as follows (Fig. 2). First, the operator manually enters a set of data relevant to the process, forming a data group or data sets. This includes data describing the physical, mechanical and operational properties of the materials to be formed, equipment data, initial CAD geometry of the object, etc. On the basis of these data, FE-simulation and experiment are carried out independently, in parallel, until the moment of getting of several variants of the results. In case of FE-simulation there can be several variants. In the case of experiments, there can be several variants of results as well, but unlike FE-simulation, this is due to the purity of experiments, not the data set. After that, the solutions are being compared to each other (validation step) and with the number (A), which characterizes the adequacy of the computer model or the accuracy of the solution using numerical simulation.

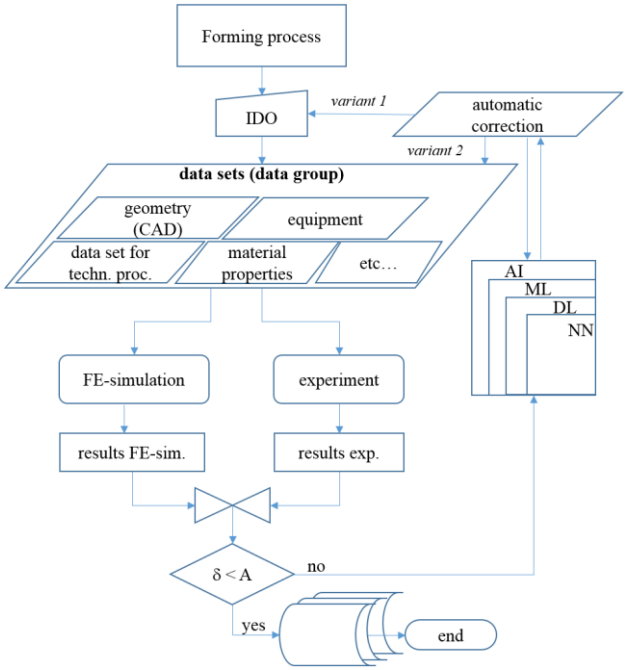

Fig. 2. Algorithm of "digital twin – technological process" development

In case of a significant deviation of the solution from the results of a full-scale experiment, the AI algorithm is activated and challenging to find out the cause of the discrepancy and offers options of manual (variant 1) or automatic (variant 2) correction of values in the data group, both for experiments and for numerical simulation. The procedure continues until a solution that meets the selected adequacy criterion is obtained. The realization of such an algorithm is impossible without timely collection and processing of information at different production stages. In the work [21] it is shown that it is possible to introduce optical 3D-scanning technologies for bolts into the production line, but the speed of 3D-model preparation and analysis compromises the procedure of full product control, as modern equipment has a higher forming rate.

The existing non-contact experimental method of strain estimation or the digital image correlation method (DIC) allows real-time recognition of the change in the position of points of the deformed specimen. One of four algorithms is applied in the strain calculation stage according to this method: subset shape function (calculates strains from the subset shape function and the deformed subset shape, with the size of the virtual strain gauge (virtual strain gauge or VSG) corresponding to the size of the subset; finite-element shape function (calculates strain based on triangulation, for which the nodes of the finite-element mesh are characteristic dark or light speckl (pixel, dot) of the pattern applied to the specimen); strain shape function (local fitting of polynomial or spline shape deformation function to displacements in order to obtain an analytical equation of the displacement field, after which deformations are calculated based on spatial derivatives of the resulting analytical equation); spline fit (global spline fitting of the displacement field) [22].

It was shown in [23] that the DIC can be applied for the Erichsen cupping test considered in this paper. However, it should be emphasized that the evaluation is performed on the outer surface of the specimen, which does not give an idea of the behavior of the material inside. For this purpose, computer modeling (simulation) is used, which gives a complete picture of the technological process. However, based on theoretical dependencies of deformation description, e.g., Green-Lagrange definition of deformation, Eq. (4), we can arrive at Eq. (5), which relates the deformation and thickness of the material, discussed in detail in [24] and [25].

$$\varepsilon = \frac{1}{2}\left(\lambda^2 - 1\right), \tag{4}$$

$$t_f = t_i \left(\frac{1}{\sqrt{(1+2\varepsilon_1)(1+2\varepsilon_2)}} \right), \quad (5)$$

where λ – ratio of the end sample length to the initial sample length; t_f and t_i – end and initial sample thickness, respectively; ε_1 и ε_2 – max. and min. principal stresses, respectively.

Deep learning and neural network algorithms are applied in the technique of DIC. In the article [26] the application of convolutional NN is considered. It is shown that training of NN should be carried out on higher quality sets of speckle patterns.

Another modern non-contact method of strain assessment is 4D-tomography. The essence of the method is the continuous process of tomography of a sample subjected to plastic deformation. In [27] the influence of strontium inclusions on the nature of fracture of hot-rolled aluminum alloy sheet specimens under uniaxial tension was studied, and strain resistance plots were determined. In most cases, ductile fracture of the specimens was established, indicating high plastic properties of the material under study. In [28], the results obtained by 4D-tomography were confirmed using the DIC technique.

4. Goals and tasks

The purpose of this study is to objectively evaluate the capabilities of modern non-contact deformation control tools available in the university laboratory and their adequacy. The task of the study is to evaluate the deformation of aluminum sheet blank by the Erichsen cupping test, and the following techniques are used:

- experimental evaluation of cupping test on specialized equipment;
- numerical simulation of the cupping process using several damage models;
- image matching or digital image correlation;
- optical 3D-scanning based on infrared or optical structured light projection.

The use of several evaluation techniques is due to the fact that during material forming the strain can refer both to the outer and inner surface of the object and to the inner region. The fact is that plastic forming of a sheet blank leads to the appearance of different thicknesses in the material, which is the result of anisotropy of properties in the material caused by inclusions, phase composition, defects such as micropores and microcracks, as well as hardening in the process of deformation. Due to these circumstances, deformation estimation would be only declarative if numerical simulation was excluded from consideration.

The application of a complex study is a more budget-friendly alternative to the most expensive 4D–tomography, because in addition to the equipment for its realization requires a powerful workstation with specialized software.

The use of DIC together with computer modeling will improve the accuracy of deformation determination on curved surface areas. Supplementing such a technique with elements of artificial intelligence (Fig. 2) will accelerate the search for the best combination of parameters. By implementing this approach, the third stage of development of the digital twin is actually realized [29], the process of building bilateral relations between the real and virtual object, which is not a finished product, but a technological process.

5. Experimental procedure

For study the evaluation of strain by non-contact method let us consider obtaining experimental data in the course of deformation of a sheet strip, 1.2 mm thick, made of aluminum alloy AMg2, according to the Erichsen cupping test scheme, l. According to GOST 10510-80 and ISO 20482, during this test the material is deformed until failure by moving the punch in opposite to gravity direction. The shape of the punch and tools is selected based on the type of material and its dimensions. The results of this test are used to determine the amount of punch displacement at which specimen failure occurred. In this study, a tool of type design 1 (according to GOST 10510-80), is used, shown in Fig. 3.

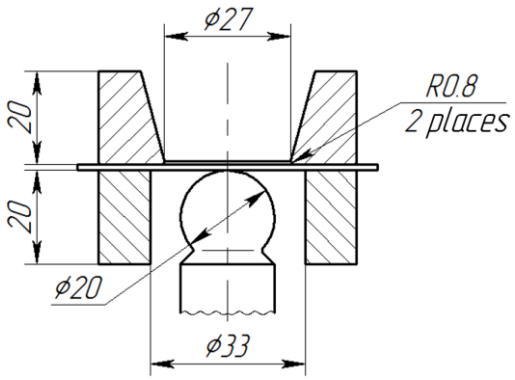

a) drawing

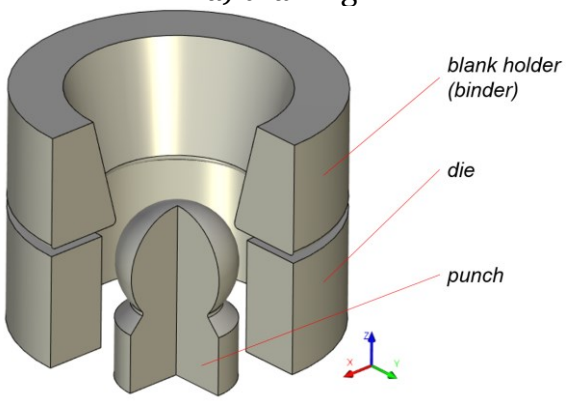

б) 3D-model, ¼ cut away

Fig. 3. Drawing of the toll with blank (a) and its 3D-model without blank (b)

During the experiments it was found out that the sample fracture occurs at a punch displacement of 11 mm, deformation force of 590 kg or 0,0059 MN, and max. thinning at the material fracture point δ = 0,4 mm. These initial data are taken as reference values and are used further for validation of numerical simulation results and optical strain estimation methods.

Fig. 4 shows the step-by-step formation of the hemisphere and the final specimen with a diametric cross-section.

6. Deformation evaluation based on simulation results

Numerical simulation of the Erichsen cupping test is performed in the QForm software. Table 1 shows the process parameters to be set. The problem was modeled in three-dimensional formulation. Table 2 shows the specified material properties. To describe the nature of the material flow, a yield curve or flow curve was used, reflecting the hardening of the material during the plastic deformation stage, described by equation (6), which coincides with the four-coefficient form of the Hensel-Spittel equation at $m_1 = m_3 = m_4 = 0$, equation (7).

Table 1. Technological parameters

Parameter	Unit	Value
Workpiece material	-	АМг2
Punch velocity	mm/s	2
Max. punch force	MN	0,1
Blank holder force	MN	0,02
Contact friction formulation	-	Levanov's friction law (m = 0,5)
Max. punch displacement	mm	12

Table 2. Physical and mechanical properties

Parameter	Unit	Value
Density	kg/m³	2 690
Thermal conductivity	W/m K	159
Heat capacity	J/kg K	963
Young module	GPa	71
Poisson's ratio	-	0,33
Thermal linear expansion coefficient	1/°C	2,4e-5

$$\sigma = k\varepsilon^n, \quad (6)$$

$$\sigma = ke^{-m_1 T}\varepsilon^{m_2}e^{-m_4\varepsilon}, \quad (7)$$

where σ – yield (flow) stress; ε – logarithmic strain; k – hardening coefficient (yield stress at $\varepsilon = 1$); n – strength coefficient; m_i – coefficients, relates the influence of temperature, strain rate and punch velocity.

Isotropic hardening conditions (by Mises) and anisotropic hardening conditions for sheet materials (by Hill-Mises) were chosen as plasticity conditions (yield criterion). The damage model was specified through the forming limit diagram (FLD), as well as through the modified Cockroft-Latham-Oh (abbr. C-L-O) model [30]. Table 3 shows the values of the coefficients of the equations of the models used in the calculations.

Table 3. Equations' coefficients

Parameter	Unit	Value
yield criterion		
r_0; r_{45}; r_{90}	-	0,1403; 0,1825; 0,2077
yield curve		
k; n = m_2	MPa; -	194,09; 0,07351
flow/forming limit diagram (FLD) damage model		
R_m; $\delta_{макс.}$	-; mm	0,178; 0,4
modified Cockroft-Latham-Oh damage model		
α; ε_{max}	-; -	0,5; 0,05

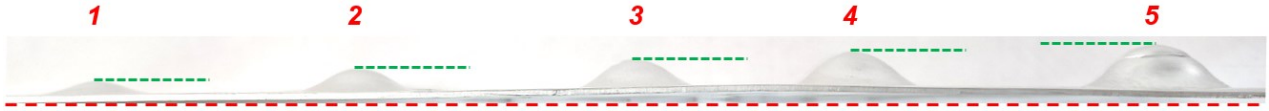

a) presentation of successive forming stages of hemisphere from the strip

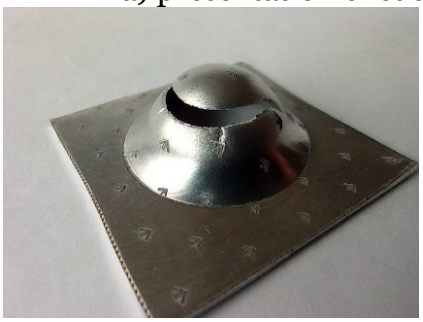

b) end form of fractured blank

c) blank's cross-section

Fig. 4. Blanks after Erichsen cupping test

According to the simulation results the technological information is obtained. The graph of deformation force against punch displacement shows the moment of load drop, which is caused by excessive thinning of the material and its subsequent failure (Fig. 5).

Fig. 6 shows the forming limit diagram and fracture regions of the material when the FLD model is used.

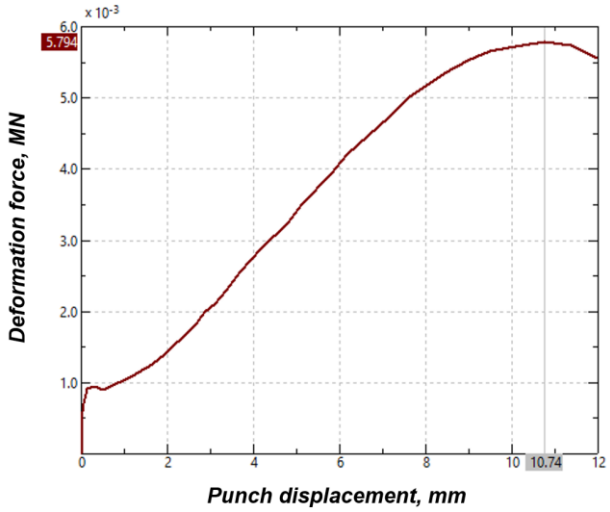

Fig. 5. Punch displacement vs. deformation force at the end of Erichsen test

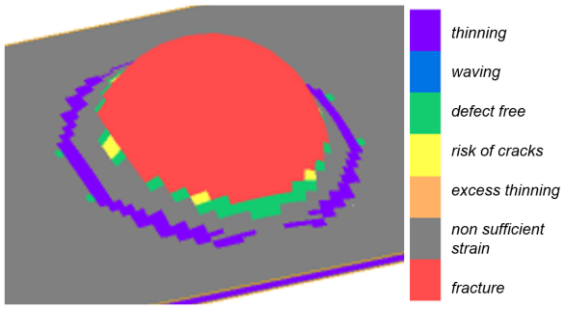

a) formability and fracture zones

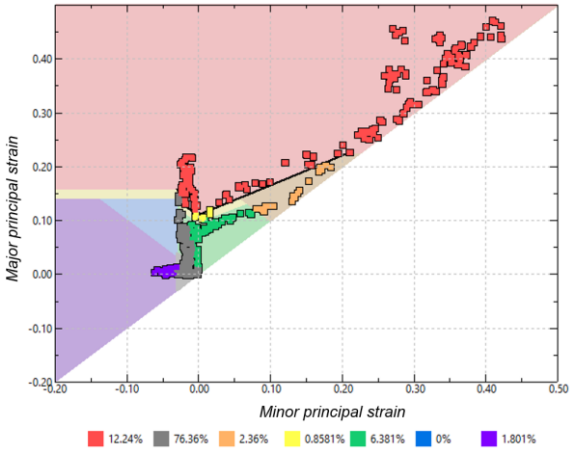

b) FLD

Fig. 6. Results of numerical simulation for FLD damage model

The fields of effective strain values and fracture regions are shown in Fig. 7. According to the model described by the FLD, it can be seen that the fracture occurs in the dome part, while it is not possible to specify a clearly defined location of the fracture initiator. At a punch displacement of 11 mm, the fracture spreads throughout the entire dome region. According to the Cockcroft-Latham-Oh model, it is possible to identify a ring-shaped area located below the dome crest, where the maximum stresses develop.

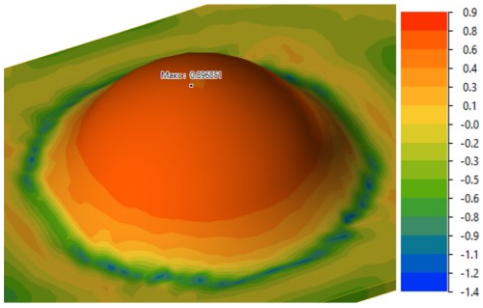

a) triaxiality (η_{max} = 0,89, red dome region corresponds the range 0,65...0,89)

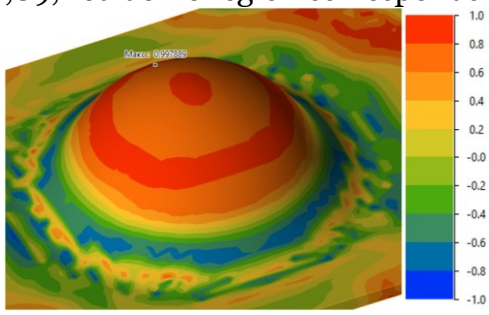

b) Lode parameter (L_{max} = 0,99, red ring region corresponds the range 0,8...0,99)

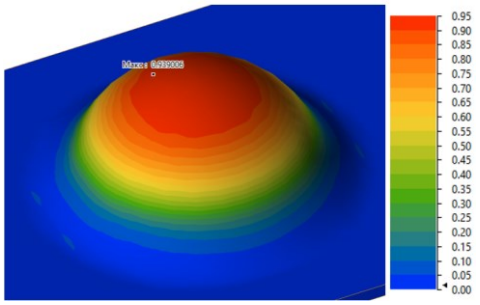

c) effective deformation field (FLD model)

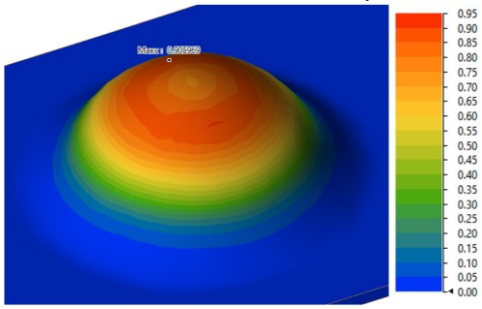

d) effective deformation field (C-L-O model)

Fig. 7. Results of numerical simulation for different damage models

The level of stress triaxiality, determined by equation (8) and reflecting the ratio of hydrostatic pressure to equivalent stress (is a function of the first and second invariants), and the Lode parameter, determined by equation (9) and is a function of the second and third invariants, indicate the compliance of the scheme with biaxial tension.

Fig. 8 shows a diagram of the relationship between the Lode parameter (via Lode angles) and the stress triaxiality as a function of the SSS of the material.

$$\eta = \frac{\sigma_m}{\bar{\sigma}} = \frac{\sigma_1 + \sigma_2 + \sigma_3}{3\bar{\sigma}}, \tag{8}$$

$$L = \frac{2\sigma_2 - \sigma_1 - \sigma_3}{\sigma_1 - \sigma_3} = \sqrt{3}\,\mathrm{tg}\,\theta, \tag{9}$$

where $\bar{\sigma}$ – effective stress (on Mieses); σ_m – hydrostatic pressure; θ – Lode angle.

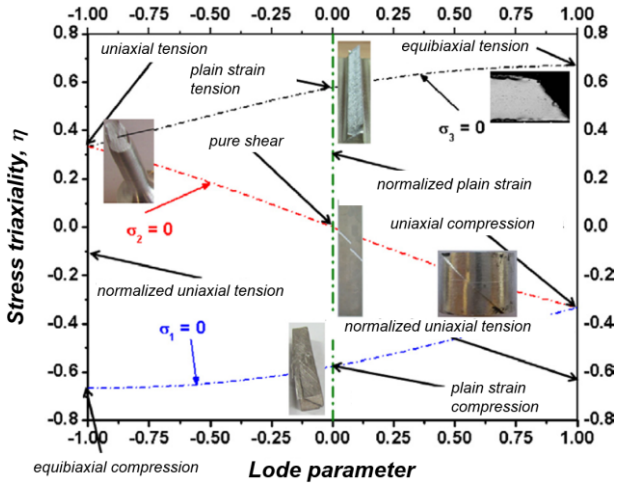

Fig. 8. Graphical correlation between Lode parameter and stress triaxiality [31]

7. Deformation evaluation based on images

Image processing can be performed using subroutines written in C++, MathLab, Java or Phyton programming languages. Machine vision algorithms have advanced significantly, and a large number of open source codes have appeared, e.g., DIC engine [32], which allow processing raster information and determining object deformation values in time. The well-known systems including hardware and software are Aramis and Argus from GOM (a division of Carl Zeiss), StrainMaster from LaVision, laserXtens from Zwick-Roell, and AutoGrid from ViALUX.

When determining strain, an important aspect is the ability to determine the location of reference points belonging to the material being deformed with high accuracy. There are two known methods to estimate the mutual location of points in space: speckle interferometry and digital image correlation (DIC). With speckle interferometry it is possible to determine the shift of point objects forming a certain image. With DIC, it is possible to correlate changes in some image, not necessarily a point image. In both cases, observation of objects over time is required, with images recorded after a certain time interval. The methods can be applied jointly, i.e., the estimation of changes in the position of point objects can be performed also by DIC algorithms.

For realization of such a combined method it is required to prepare the sample surface and to draw a special pattern on it. For example, for realization of the method of deforming grids it is required to draw a pattern on the sample in the form of a grid formed by intersecting parallel lines with known cell parameters. In contrast, the speckle interferometry method requires the creation of a point pattern with a unique, non-repeating distribution pattern. The main requirements for the pattern are the following: non-glare surface, points of different diameters and its chaotic distribution. Figure 9 shows variants of pattern preparation with non-glare-free (left) and glare-free (right) surfaces. To perform DIC, it is enough to create a certain pattern, i.e. a drawing with repeating elements.

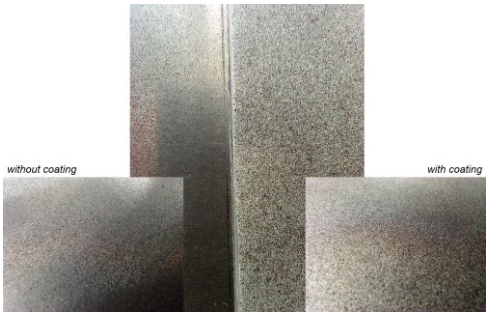

Fig. 9. Pattern on the blanks' surfaces, prepared using sprayed black paint

In both cases, the necessary patterns can be created either manually or by engraving methods, including non-contact laser engraving. Fig. 10 shows some samples of a computer prepared templates or pattern in the upper row, and samples with the laser engraved pattern applied in the lower row.

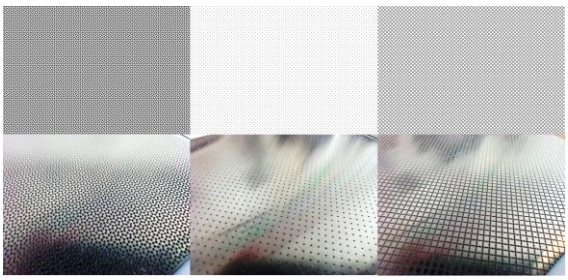

Fig. 10. Patterns on the blanks, prepared by laser engraving

During the tests, continuous video recording in FullHD mode (resolution of 1980 x 1080 and higher) is performed. After the video recording is obtained, it is storyboarded, saving, for example, every tenth frame. Then in the GOM Correlate software the obtained set of frames is loaded to the frame scale and the recognition of point movements with strain estimation is carried out for all the images-frames in automatic mode (Fig. 11). Bicubic interpolation of subpixels is used. In case of insufficient information the program shows displacement of only some points (Fig. 11a). It is also possible to additionally compare surface points, enter reference points for matching, exclude redundant points from the image analysis area or region of interest (abbr. ROI, Fig. 11b).

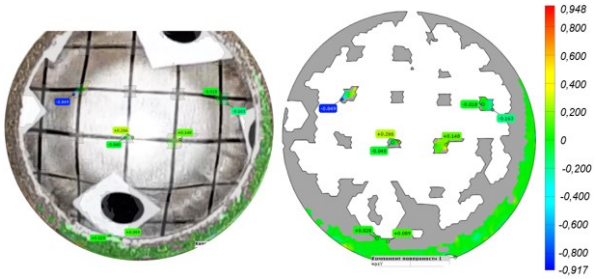

a) field of equivalent strains

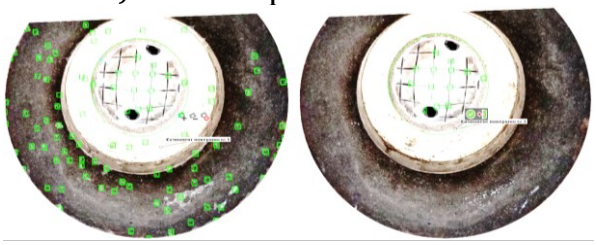

b) assigning points to the surface (left) and excluding redundant points (right) from the ROI

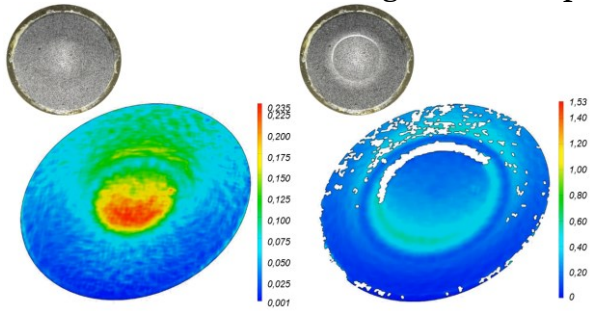

c) field of equivalent strains (left – mid-process; right – end-process, after crack building) and views of real blanks during deformation stage

Fig. 11. Preparing and recognition the blank surface applying DIC and SPECKL

In case of successful recognition, a color scheme or a color map of displacements/deformations of individual points is plotted on the surface of the ROI (Fig. 11c).

8. Deformation evaluation based on 3D-scanning

After the experiments, the failure blanks were subjected to optical 3D-scanning using a RangeVision Neopoint 3D-scanner, which operates on the infrared (IR) structured light projection, realized on laser diodes, guaranteeing measurement accuracy up to 50 μm. Before scanning, a matting spray like developer was applied to the samples to create a uniform reflection coefficient over the entire surface of the object. Scanning was carried out in scanning mode on a rotary table with a rotation angle step of 30°, which allows to create 12 scans, on the basis of which a polygonal stl-model is reconstructed. The average error value at the scan stitching stage was 51 μm. Fig. 12a shows the stl-model of one of the samples presented from different angles.

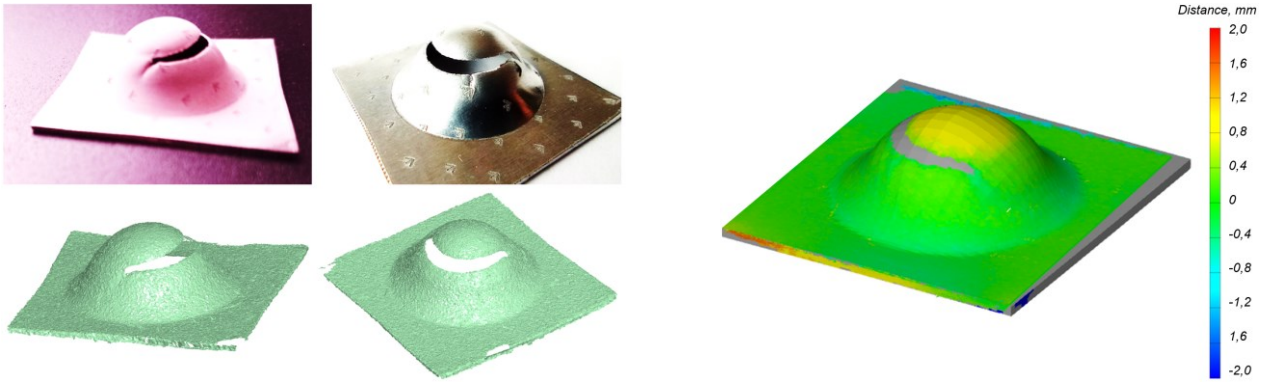

a) comparison of the real sample after Erichsen cupping test (upper line) with its digital geometrical twin (lower line)

b) distances between two polygonal stl-models

Fig. 12. Comparing the end polygonal stl-models

Comparing the models after numerical simulation and 3D scanning in the GOM-Correlate program, it can be noted that the maximum deviation is observed in the dome part of the sample and is Δ = +0,85 мм (Fig. 12b). In this case, it is possible to correct the displacement of the punch at which the results were uploaded, i.e. 10,74 mm + 0,85 mm = 11,59 mm (according to Fig. 5).

On the other hand, it is also possible to reach this value through numerical simulation, i.e., to reduce the deviation value (Δ) by defining a constant time step, which will increase the calculation time, but in addition to obtaining a more accurate value of height, it will also make it possible to determine the value of the limiting deformation more accurate. The areas shown in gray are those that are partially excluded from consideration. They show that the dimensions of the original workpiece used for numerical modeling were slightly larger than the dimensions of the experimental specimen.

This was due to the need to obtain additional information on the SSS of material under the blank holder. In the experiment, the blank holder contacted not always over the entire area of the contact surface, which resulted in the retraction of a part of the workpiece into the area of plastic deformation.

9. Conclusions

Application of experimental non-contact methods of strain estimation will considerably simplify the procedure of strain value estimation at manufacturing of complex sheet parts by metal forming operations. Nowadays, such methods are the results of approbation of a new technology and methodology, according to which they can be used for cases of laboratory

study of mechanical properties, since they require preparation of the blank surface, availability of a calibrated system and special software. It is extremely difficult to apply them to control deformation of complex sheet parts during the process run.

To date, the most reasonable is the combined use of numerical simulation tools and subsequent mechanical testing using, for example, DIC.

The tasks of Erichsen testing of a sheet blank made of aluminum alloy AMg2, followed by numerical simulation of the process and speckle-DIC method of strain assessment based on the results of video recording of the experiment were successfully performed and showed that numerical simulation requires information about the coefficients included in the calculation models of material flow and fracture, and speckle-DIC requires specimen preparation. The additional application of optical 3D-scanning will allow the introduction of quality control information on the resulting specimen geometry after testing. The generalized results of experimental studies and numerical simulation can be used to create AI aimed at developing a digital twin of the technological process.

References

[1] https://aat.moscow/avtomobilnaja-promyshlennost/ (date of last access 17.10.2023).

[2] http://www.stamping.by/industry/shtampovannye-izdeliya-iz-metalla (date of last access 20.10.2023).

[3] https://3dprintingcenter.net/desktop-metal-introduces-figur-g15-a-new-technology-for-digital-sheet-metal-forming-which-has-nothing-to-do-with-3d-printing/ (date of last access 20.10.2023).

[4] Xu, D., Chen, J., Tang, Y., & Cao, J. (2012). Topology optimization of die weight reduction for high-strength sheet metal stamping. International Journal of Mechanical Sciences, 59(1), 73–82. doi:10.1016/j.ijmecsci.2012.03.006

[5] https://www.youtube.com/watch?app=desktop&v=J-SPyER7tFs (date of last access 20.10.2023).

[6] Azamirad, G., & Arezoo, B. (2016). Topology optimization of stamping die components using evolutionary structural optimization method. Proceedings of the Institution of Mechanical Engineers, Part B: Journal of Engineering Manufacture, 231(4), 690–698. doi:10.1177/0954405415597630

[7] Su, T. C., He, T., Yang, R., & Li, M. (2021). Topology optimization and lightweight design of stamping dies for forming automobile panels. https://doi.org/10.21203/rs.3.rs-791304/v1

[8] Petrov M.A., Urzhumov P.N., Numerical Simulation of the Hot Bulk Forming Process of the “CAP” Like Forming with Topology Optimization of the Tool Set, Russian Internet Journal of Industrial Engineering, 2022, Vol. 9(2), pp. 3–9.

[9] Effect of ductile damage evolution in sheet metal forming: experimental and numerical investigations / F. Abbassi, O. Pantale, S. Mistou, A. Zghal, R. Rakotomalala // Key Engineering Materials. 2010. № 446. C. 157–169. DOI: 10.4028/www.scientific.net/KEM.446.157

[10] Kraft- und Deformationscharakteristika beim Umformen eines Stahlblech-Verbundwerkstoffs / M. Petrov, S. Guk, J. Bast, P. Petrov // Lightweight Design. 2012. №5. C. 50–57. DOI: 10.1365/s35725-012-0023-5

[11] Definition of area of the maximum shear deformations for CFRP samples on Iosipescu method, with use of optical system of measurements / A.V. Ilichev, A.M. Gubin, A.R. Akmeev, N.V. Ivanov // Trudy «VIAM». 2018. №6. pp. 99–109. DOI: 10.18577/2307-6046-2018-0-6-99-109

[12] Tretyakova T.V. Ocenka vlijanija slozhnogo naprjazhenno-deformirovannogo sostojanija na projavlenie jeffekta Portevena-Le Shatel'e v Al-Mg splave // Ajerokosmicheskaja tehnika, vysokie tehnologii i innovacii. 2021. Vol. 2. pp. 206–209.

[13] Besnard G., Hild F., Roux S. “Finite-element” displacement fields analysis from digital images: Application to Portevin-Le Châtelier // Experimental Mechanics. 2006. №46(6), C. 789–803. DOI: 10.1007/s11340-006-9824-8

[14] Agha A., Abu-Farha F. A Method for Measuring In-Plane Forming Limit Curves (FLC) using 2D Digital Image Correlation // SAE MobilityRxiv™ Preprint. 2023. URL: https://mobilityrxiv.sae.org/preprint/a-method-for-measuring-in-plane-forming-limit-curves-flc-using-2d-digital-image-correlation--sae-pp-00322 (date of last access 03.08.2023). DOI: 10.47953/SAE-PP-00322

[15] In situ opredelenie nepreryvnoj jevoljucii v prostranstve i vo vremeni deformacionnyh polej na stal'noj plastine s koncentratorom naprjazhenij / V.A. Vlasov, A.S. Plyaskin, A.A. Klopotov [etc.] // Modern construction materials and technologies: Conference Proceedings of the III International Conference, Kaliningrad, 26–29 May 2020 / M.A. Dmitrieva, eds., Vol. 3, Kaliningrad: Immanuil Kant Baltic Federal University, 2021. pp. 164–172.

[16] Strungar E.M., Lobanov D.S. Development of the digital image correlation (DIC) method for mechanical testing at elevated temperatures. PNRPU Mechanics Bulletin, 2022, no. 3, pp. 147-159. DOI: 10.15593/perm.mech/2022.3.15

[17] Kibitkin V.V., Solodushkin A.I. Uvelichenie ploshhadi kontrolja pri izmerenii deformacii tverdogo tela metodom korreljacii cifrovyh izobrazhenij // Izvestija vuzov. Fizika. 2021. № 64. pp. 32–37. DOI: 10.17223/00213411/64/4/32

[18] Numerical and Experimental Investigation of Deep Drawing of Sandwich Panels / S. Tipalin, M. Petrov, B. Saprikin, N. Kosatchyov, N. Shpunkin, P. Petrov // Key Engineering Materials. 2014. Vols. 611-612, C. 1627–1636. DOI: 10.4028/www.scientific.net/KEM.611-612.1627

[19] Popov E.A. Osnovy teorii listovoj shtampovki. M.: Mashinostroenie, 1977. 278 p.

[20] Russel S.J., Norvig P., Artificial Intelligence. A modern Approach, 2nd edition, 2003, Upper Saddle River, NJ: Prentice Hall, p. 1080.

[21] Petrov M.A., El-Deeb I.S.A., To the development of the algorithm for the inline inspection of the geometric and technological parameters on the example of cold bulk forging of a bolt blank, Kuznechno-shtampovochnoe proizvodstvo. Obrabotka materialov davleniem, №4, 2020, pp. 39–48

[22] https://idics.org/guide/DICGoodPracticesGuide_ElectronicVersion-V5g-181022.pdf (date of last access 20.10.2023).

[23] M. Aydin, X. Wub, K. Cetinkaya, M. Yasar, I. Kadi, Application of Digital Image Correlation technique to Erichsen Cupping Test, Engineering Science and Technology, an International Journal, 2018, Vol. 21, C. 760–768.

[24] Van Mieghem, B., Ivens, J., & Van Bael, A. (2016). Consistency of Strain Fields and Thickness Distributions in Thermoforming Experiments Through Stereo DIC. Experimental Techniques, 40(5), 1409–1420. doi:10.1007/s40799-016-0143-4

[25] Gonzalez, M. M., Lutes, N. A., Fischer, J. D., Woodside, M. R., Bristow, D. A., & Landers, R. G. (2019). Analysis of geometric accuracy and thickness reduction in multistage incremental sheet forming using digital image correlation. Procedia Manufacturing, 34, 950–960. https://doi.org/10.1016/j.promfg.2019.06.105

[26] Boukhtache, S., Abdelouahab, K., Berry, F., Blaysat, B., Grédiac, M., & Sur, F. (2021). When Deep Learning Meets Digital Image Correlation. Optics and Lasers in Engineering, 136, 106308. doi:10.1016/j.optlaseng.2020.106308

[27] Samei, J., Sadeghi, A., Mortezapour, H., Salavati, S., Amirmaleki, M., Pekguleryuz, M., & Wilkinson, D. S. (2020). 4D X-ray tomography characterization of void nucleation and growth during deformation of strontium-added AZ31 alloys. Materials Science and Engineering: A, 797, 140081. doi:10.1016/j.msea.2020.140081

[28] Nazari-Onlaghi, S., Sadeghi, A., Karimpour, M., & Pekguleryuz, M. (2021). Fracture micro-mechanisms in hot-rolled AZ31 and AZ31-Sr magnesium alloys. Materials Science and Engineering: A, 812, 141107. doi:10.1016/j.msea.2021.141107

[29] Kitain L. The New Age of Manufacturing: Digital Twin Technology & IIoT, The New Age of Manufacturing, 2018, http://www.innovation4.cn/library/r46394 (date of last access 20.10.2023).

[30] Stebunov S., Vlasov A., Biba N. Prediction of the fracture in cold forging with modified Cockcroft-Latham criterion // Procedia Manufacturing. 2018. № 15. С. 519–526. DOI: 10.1016/j.promfg.2018.07.264

[31] Lou Y., Yoon J.W., Huh H. Modeling of shear ductile fracture considering a changeable cut-off value for stress triaxiality // International Journal of Plasticity. 2014. № 54. С. 56–80. DOI: 10.1016/j.ijplas.2013.08.006

[32] https://www.sandia.gov/ccr/software/digital-image-correlation-engine-dice/ (date of last access 20.10.2023).